swiss physical society

Nr. 73, Juli 2024

SPG Mitteilungen
Communications de la SSP

Auszug - Extrait

Progress in Physics (101)

Scalable optical memories in MEMS vapor cells for quantum networking

Roberto Mottola, Gianni Buser, and Philipp Treutlein
Departement Physik, Universität Basel, Klingelbergstr. 82, 4056 Basel

DOI: 10.5281/zenodo.13208932

Progress in Physics (101)

Scalable optical memories in MEMS vapor cells for quantum networking

Roberto Mottola, Gianni Buser, and Philipp Treutlein
Departement Physik, Universität Basel, Klingelbergstr. 82, 4056 Basel

The roadmaps towards a quantum internet [1, 2] envision revolutionary breakthroughs, like its classical analog had in our everyday lives. Quantum networks promise to enable private communication between remote parties through the distribution of provably secure cryptographic keys, relying on the laws of quantum physics [3]. Furthermore, they could help overcome scalability concerns in quantum computers, as well as allowing the exchange of computation results in the form of qubits, or sharing entanglement between distant recipients [4]. Quantum metrology could also benefit from quantum networks through enhanced precision by combining the measurements of remote quantum sensors in a network [5, 6].

Quantum networks are composed of nodes that can store and process quantum information. These network nodes are linked via quantum channels. Through these flying qubits, typically single photons, can be sent either to directly transfer quantum information, share entanglement, or synchronize probabilistic operations [7]. First realizations of elementary networks for entanglement distribution have been demonstrated in a variety of platforms [8]. In [9] entanglement between two remote single atoms each trapped in a cavity was generated and subsequently manipulated by local qubit rotations. Event-ready Bell tests have been performed to verify the entanglement of two trapped atoms at separated nodes [10]. Hybrid approaches were pursued as well, as in [11] where two different rare-earth ion based quantum memories operating at different wavelengths were entangled through spontaneous parametric downconversion (SPDC) photons. Moreover, a truly heterogeneous interconnect between a cold atomic ensemble and a rare-earth doped crystal was successfully demonstrated making use of quantum frequency conversion [12]. Recently, the first three-node networks for entanglement distribution were realized. This is the state-of-the-art. In cold atomic ensembles, entanglement of nodes was achieved through three-photon interference [13]. Further, the heralded generation of a GHZ state across three independent nitrogen vacancy centers in diamond nodes was reported on in [14], constituting a small network with quantum memories at the nodes capable of storing and processing quantum information. Subsequently, quantum teleportation between non-neighboring nodes was also shown in that system [15].

Quantum Network Building Blocks

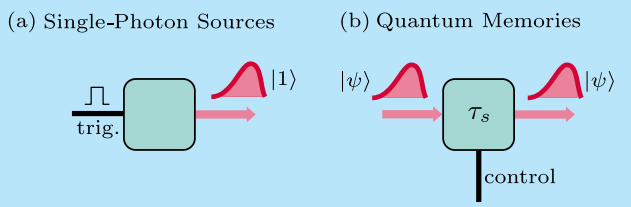

(a) An ideal single-photon source is an apparatus that emits exactly one photon. The distinction can be made between deterministic sources, where the photon is produced at the push of a button, and probabilistic ones, which emit spontaneously, at random points in time. The latter type can be just as useful given that photons are systematically produced in pairs. In that case one can be detected to herald the generation of the other [16].
(b) A quantum memory can be described as a device that takes an input quantum state from a single photon and faithfully preserves it in time. (If desirable, it might also perform an operation on the input state.) At a later point in time, this device should be able to re-emit the single photon in said quantum state [17].

Optical interconnects that reversibly map quantum states between matter and light are fundamental for the realization of quantum networks. Single-photon sources and quantum memories thus constitute their building blocks. Realistic, large-scale implementations of quantum networks pose demanding challenges for these elementary components. They should be easy to operate in environments outside of a laboratory, while at the same time being scalable and, preferably, easy to mass-produce.

Due to their simple atomic level structure and strong optical transitions, alkali metals are a convenient platform for implementing quantum memories. Significantly, their high vapor pressure allows for operation at room temperature. This results in relatively simple setups without the experimental overhead required by cryogenic or ultra-high vacuum systems. Additionally, bandwidths of hundreds of MHz to single GHz can be reached in hot vapor memories, allowing them to be matched with high quality single-photon sources such as semiconductor quantum dots [18 - 20] or SPDC sources [21, 22].

Hot alkali vapors are generally contained in vapor cells, which can range from conventional glass-blown cells, com-

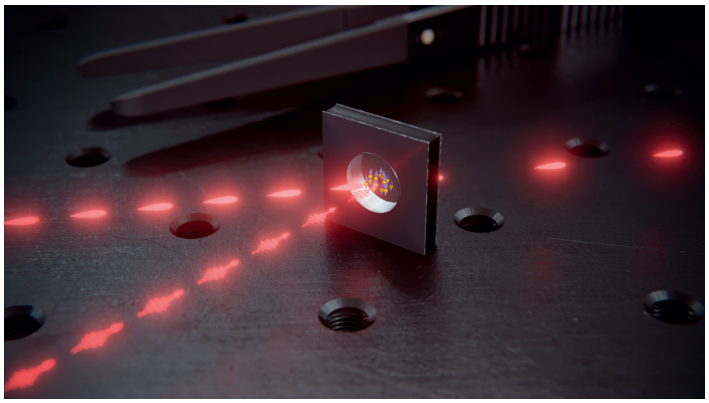

FIG. 1. Artist's depiction of an optical memory implemented in a MEMS vapor cell. The 2 mm thin cell can store weak light pulses consisting on average of a single photon and re-emit them at a later point in time.

monly used for spectroscopy, to wafer-scale microfabricated cells [23]. Up to now, microfabricated cells were used predominantly in the field of quantum sensors, for compact atomic clocks, magnetometers and gyroscopes [24]. So far, no quantum memory was implemented in MEMS (micro-electromechanical system) cells. Nevertheless, the MEMS fabrication capabilities are promising for the development of scalable quantum networks – they could enable spatial multiplexing of memories with hundreds of independent vapor cells on a single wafer, and satisfy the miniaturization requirements of satellite-borne applications [25].

Storing Single Photons in Hot Vapor

A prominent choice for storage schemes in atomic ensembles are three-level lambda-systems as depicted in Fig. 2. Lambda systems are composed of two metastable ground-states and one excited state. The long coherence times of the atomic ground states aid in preserving the stored information. Initially, the atoms are prepared in the ground state $|g\rangle$. The incoming single photon is chosen to be resonant to the $|g\rangle \rightarrow |e\rangle$ transition. A strong control pulse, resonant to the second leg of the lambda ($|s\rangle \rightarrow |e\rangle$), is shun on the ensemble as the single-photon arrives, which maps it to a spin wave between the two ground states. In other words, the incoming photonic excitation is mapped onto a shared coherent excitation of the atoms. This process can be represented as

$$|1\rangle_{ph} \otimes |g_1, g_2, ..., g_N\rangle \leftrightarrow |0\rangle_{ph} \otimes \frac{1}{\sqrt{N}} \sum_{j=1}^{N} |g_1, g_2, ..., s_j, ..., g_N\rangle .$$

The resultant atomic excitation is known as Dicke state, or as W state in the field of quantum information theory, which is particularly robust against particle losses [26]. In the experiments described below, the excitation is stored in an entangled state containing on the order of a billion atoms.

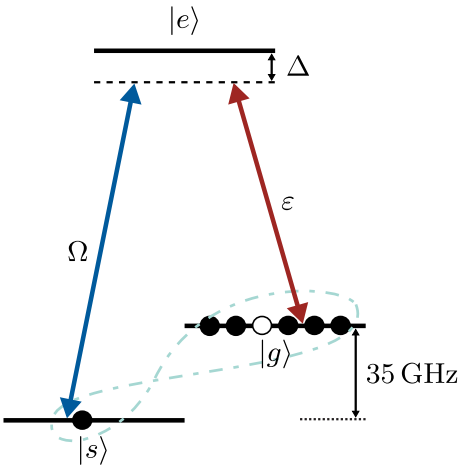

FIG. 2. Lambda-scheme used for light storage in the atomic ensemble. The atoms are initialized in the ground state $|g\rangle$. The ground-state splitting determines how easy it is to filter out the control pulse after the memory and sets an upper limit to the input's bandwidth. The signal input ε and the control pulse Ω are on two-photon resonance. The detuning Δ is optimized empirically. The incoming photon is mapped onto a spin wave between the two ground states.

Depending on the exact operating regime (determined by the power and detuning of the control pulse) the underlying physical process varies. In our implementations the relevant phenomenon is called electromagnetically induced transparency [27], which can be understood as an interference of different absorption paths that prevents the excitation of the atom into the short-lived state $|e\rangle$, instead storing the photon in the ground state. The read-out process works through time-reversal. Once a photon is stored, it can be read-out at a later point in time by applying a second control pulse. Since the phenomenon is based on a collective effect, due to constructive interference of the single atoms, the re-emission of the photons is directional along the same direction as the input (contrary to fluorescence which is isotropic). This important detail makes the process particularly convenient for collecting the output.

Implementing a quantum memory ground-state scheme in a warm atomic ensemble comes with some major challenges. At room temperature, all the ground states of alkali metals are equally populated. The strong control pulse used for reading in and out of the memory can couple to these states and produce additional, typically thermal, light, e.g. through spontaneous Raman scattering. These noise photons can be generated with the same frequency and polarization as the signal photon and can't necessarily be filtered out after the memory. It is therefore imperative to initialize the atoms in the desired state to inhibit these processes. However, even for a perfect initial state preparation, the control pulse can couple to state $|g\rangle$ and lead to four-wave mixing [21, 28, 29]. Furthermore, real atoms have a far more complex level structure than the idealized three-level scheme needed for storage. These additional states can contribute to the read-out noise as well as adding spurious absorption channels, which absorb the incoming photon incoherently without storing it [30, 31]. A clever choice of scheme is necessary, e.g. by exploiting selection rules or engineering the level structure through the Zeeman effect, to suppress such possible detrimental processes.

Recently, our group demonstrated the successful suppression of noise processes in a rubidium ground-state memory, leading to the first storage and retrieval of high-bandwidth single photons in such a system [32]. That study showed the feasibility of interfacing hot vapor memories with single photons by measuring non-classical number statistics of the memory output. An important challenge is to realize such a memory in a microfabricated MEMS cell.

MEMS Vapor Cell Memory

In [33], we reported the first experiment demonstrating storage and retrieval of light in a microfabricated rubidium vapor cell. The cell shown in Fig. 3(b) was originally fabricated by the University of Neuchâtel for miniaturized atomic clocks [34]. By applying a tesla-order static magnetic field, a clean three-level lambda scheme was isolated – this reduces the spurious effects of other energy levels. In the so called hyperfine Paschen-Back regime the energy splittings induced by the Zeeman shift are larger than the hyperfine splittings. The magnetic interaction dominates and the hyperfine interaction can be treated as a perturbation, leading to the decoupling of the nuclear spin ***I*** and the total angular momentum of the electron ***J***. This allows optical control and addressing single transitions even in a Doppler broadened medium. For further details about the Paschen-Back regime we refer the reader to [35].

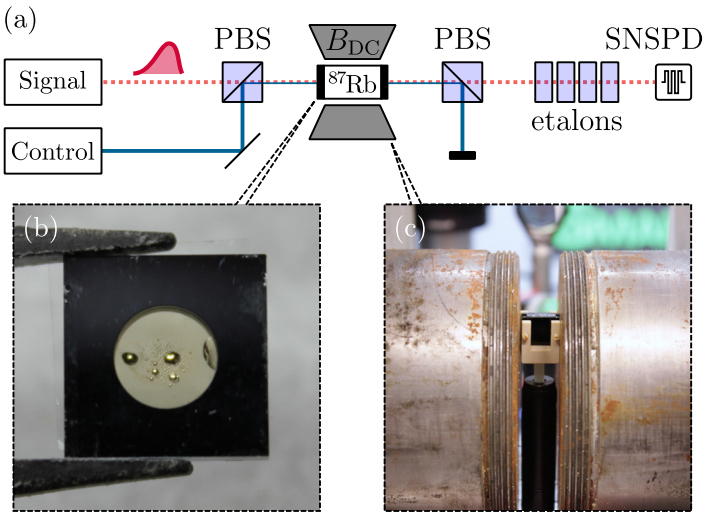

FIG. 3. (a) Sketch of the experimental setup. A strongly attenuated laser generates the single-photon-level signal pulses which are overlapped with the control pulses on a polarizing beam splitter (PBS). The heart of the memory – a rubidium MEMS cell – is placed in a static, tesla-order magnetic field B_{DC}. The memory read-out is "cleaned" by suppressing the control pulse through polarization and spectral filtration. The memory output is finally detected with a superconducting nanowire single-photon detector (SNSPD).
(b) Front view of the microfabricated vapor cell. The contained ^{87}Rb can be recognized as droplets on the cell window. By homogeneously heating the cell windows the Rb condenses on the side walls, "cleaning" the windows.
(c) An electromagnet is used to generate the strong magnetic field. The cell is placed between the ferromagnetic cores, where the field is most homogeneous. For future developments compact permanent magnets are envisioned to reduce the package size drastically (similar to what is used in [36]).

The efficiency of a quantum memory scales with the optical depth of the vapor. However, for a vapor cell with a thickness of merely 2 mm, the optical depth is negligible at room temperature. In fact, for alkali metal atoms the vapor pressure has a strong dependence on temperature. By heating the MEMS cell the atom number density thus increases, resulting in a higher optical depth. Hence, good memory efficiencies can be reached even in thin cells. In this particular case the cell was heated to about 90°C by illuminating it with infrared lasers.

A schematic representation of the experimental setup is shown in Fig. 3(a). The signal is generated by pulsing and attenuating a laser to the level that each pulse contains only one photon on average. These pulses are shaped to have a FWHM of about 1 ns and to resemble the envelope of photons from a downconversion source. The necessary strong control pulses are generated by an optically amplified laser. Signal and control pulses are timed to arrive simultaneously at the vapor cell.

Once the input light pulse is stored, we wait for a storage time of 80 ns before applying the read-out pulse. After retrieval, one major experimental challenges is to discriminate the 10^8 – 10^9 photons constituting the control pulse from the single reemitted photon. For this purpose the memory output needs to be filtered in polarization and frequency. Calcite prisms with excellent polarization extinction ratios of at least 8 orders of magnitude are used to separate the orthogonally polarized control. Furthermore, a cascade of etalons is used for spectral filtration. The frequency difference between signal and control is given by the hyperfine splitting of the atomic species (and the applied magnetic field). In total, the control light is suppressed by more than 15 orders of magnitude, while the signal transmission through the whole setup stays at around 20 %. The detection of the memory output is performed with superconducting nanowire single-photon detectors.

A typical arrival-time histogram for the storage of laser pulses attenuated to the single-photon level in the MEMS cell is shown in Fig. 4(b). Before each storage attempt, the atoms' initial state is prepared by optical pumping.

Zero time delay here corresponds to the arrival time of photons that are not stored in the memory, simply leaking through to the detector. After approximately 80 ns, the read-out control pulse is applied. The photons retrieved from the memory constitute the second peak. In order to estimate the read-out noise generated by the memory, a second measurement is performed with the signal input physically blocked. From the counts accumulated within the retrieval time-window (shaded area in the figure) of both measurements, the key figures of merit of the memory can be computed. A signal-to-noise ratio SNR = 7.9(8) and a memory efficiency $\eta^{80\ \mathrm{ns}}$ = 3.12(17) % were achieved. The memory efficiency is the fraction of noise-corrected counts detected in the retrieval time window with respect to the total amount of storage attempts that were made during the integration time. Although, this latter quantity might seem low, it specifies an end-to-end efficiency that includes all experimental losses and inefficiencies along the optical path. Correcting for said losses yields an internal efficiency (extrapolated to arbitrarily short storage times) η_{int} = 24(3) %. This value, which describes the efficiency of the physical process itself and is often the quantity cited in literature, is reasonably close to the theoretical maximum [37] for an optical memory with the given optical depth.

By repeating the experiment for various storage times, a change in efficiency can be observed. From the efficiency drop towards longer storage times (see Fig. 4(c)) the memory lifetime can be extracted. Commonly, the memory lifetime is defined as the storage time at which the efficiency drops to 1/e of its maximum value. For this first memory implementation in a MEMS cell, a lifetime of 224(8) ns was measured.

Outlook

Different applications require different sets of vapor cell parameters. The proof-of-principle experiment presented here was implemented with a microfabricated cell that was designed for atomic clocks. This leaves ample room for improvement in the next iteration. By optimizing the cell design and its filling specifically for quantum memories, several of the current limitations will be overcome and the performance – in terms of signal-to-noise ratio, efficiency, and lifetime – improved.

The initial state preparation of the atoms is crucial for minimizing the read-out noise. If additional states, especially the storage state $|s\rangle$, remain populated, the strong control pulse can couple to them and generate read-out noise. If the Rb number density is too high, the state preparation becomes less efficient due to an effect called radiation trap-

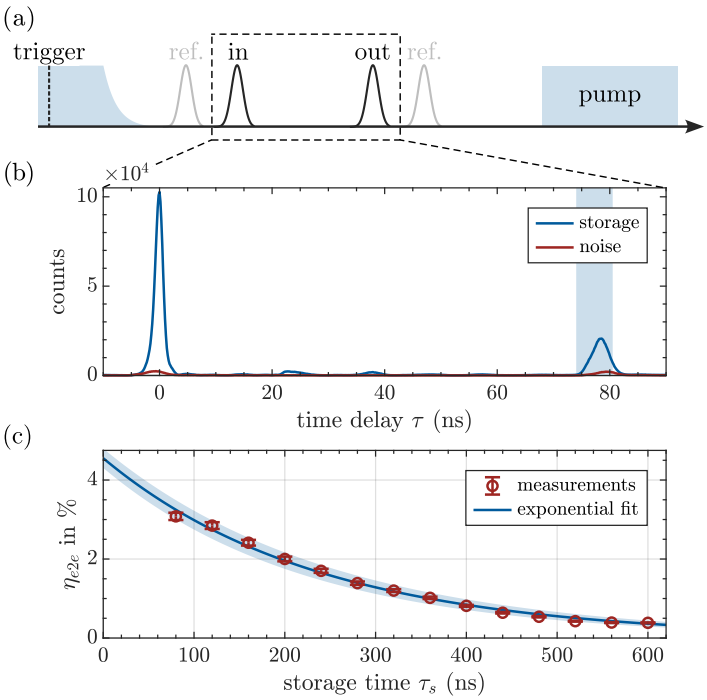

FIG. 4. (a) Pulse pattern applied to the memory. After receiving a trigger, the pump laser initializing the atoms is switched off. Two control pulses, separated by the storage time, are applied for the read-in and read-out of the memory. The signal input is timed to arrive at the atoms together with the first control pulse.
(b) Typical arrival-time histogram of a storage experiment with an integration time of about 1 min (blue trace). The peak at zero time delay comes from photons that leak through the memory during read-in without being stored. After approximately 80 ns, the read-out control pulse is applied. The photons retrieved from the memory constitute the second peak. All detection events within the shaded area – the retrieval time-window – contribute to the memory efficiency and signal-to-noise ratio. A second measurement, where the signal input is physically blocked, is performed to estimate the noise contribution (red trace).
(c) By varying the storage time, the memory lifetime can be extracted from the decrease in efficiency. The change in efficiency is well fit by an exponential decay, suggesting the lifetime is limited by loss processes.

ping [38]. When optically pumping a vapor, an excited atom emits a photon when relaxing back into the desired ground state. Under moderate conditions, these photons exit the medium, but in a sufficiently dense vapor these photons can be reabsorbed by other atoms, leading to a process which competes with depletion pumping and makes it less efficient. By adding a buffer gas, e.g. N_2, molecular ro-vibrational degrees of freedom provide the atoms with a non-radiative relaxation channel through collisions. This process, known as quenching, improves the initial atomic polarization at high density, reducing the read-out noise [39], and potentially reaching a regime as in [32], where actual single-photon storage was demonstrated.

An alternative to increasing the cell's optical depth without simultaneously increasing the alkali number density is to provide a longer optical path through the atomic vapor. The small size of MEMS vapor cells is key to their good scalability. By engineering cells where the light is internally routed through the vapor by reflections within the cell, path lengths of the order of 10 mm could be achieved [24].

In a hot vapor the atoms are in motion. A current limitation of the memory lifetime are the atoms leaving the interaction volume during the storage time. The later the control pulse is applied for readout, the less atoms contributing to the collective coherent excitation are addressed. Matching the vapor cell's inner diameter to the transverse beam profile ensures that the atoms are confined within the interaction volume. The atoms collide with the cell walls, but remain addressable as they bounce back into the control beam's path. To ensure that the atoms' collisions with the cell walls do not scramble the stored information, spin-preserving coatings [40], such as paraffin wax, must be applied to the walls. An improvement of three to four orders of magnitude in lifetime, depending on the number of collisions for which the spin is preserved, is expected with this technique. Beyond that, second-long storage times have been demonstrated in hot vapors by applying elaborate schemes to combat decoherence [41].

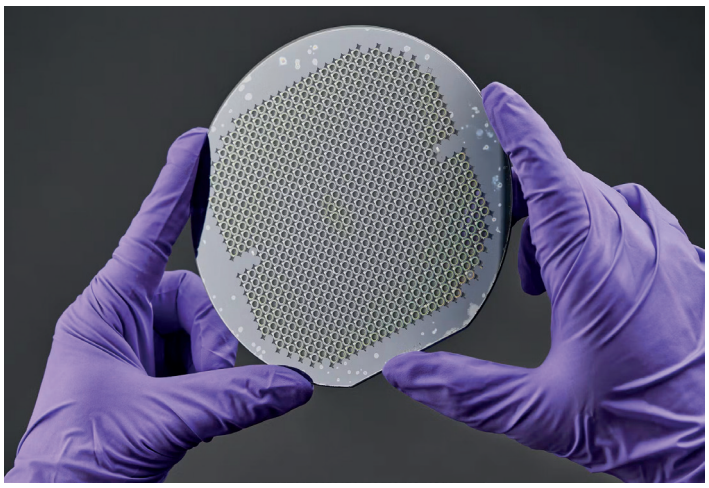

FIG. 5. Hundreds of vapor cells can be fabricated on a single wafer, potentially constituting hundreds of independent quantum memories. Photo courtesy of CSEM Neuchâtel.

Recently, the *Scalable High Bandwidth Quantum Network* (*sQnet*) project started, funded through the Quantum Transitional Call by the State Secretariat for Education, Research and Innovation (SERI). It involves a collaboration between the Treutlein and Warburton groups at the University of Basel and the CSEM in Neuchâtel, combining atomic vapor quantum memories, state-of-the-art single-photon sources based on semiconductor quantum dots, and the expertise in fabricating wafer-scale vapor cells as well as waveguides on-chip. The goal of this collaboration is to create a scalable platform for high-bandwidth quantum networks based on high performance elements. A hybrid optical interconnect in which single photons emitted by semiconductor quantum dots are stored in compatible quantum memories implemented in tailored MEMS cells will be realized by combining these elements. A further step will be to use on-chip nonlinear optics to efficiently convert the near-infrared single photons to telecom wavelengths to drastically reduce the losses in transmission through optical fibers. With such a toolbox, first quantum networking tasks such as sharing entanglement between quantum memories over telecom links could be implemented. Demonstrating the feasibility of a scalable quantum networking platform operating with high efficiency and at high bandwidth would pave the road for more complex networking tasks and scaling up to multiple nodes.

References

[1] H. J. Kimble, The quantum internet, *Nature* **453**, 1023 (2008).
[2] S. Wehner, D. Elkouss, and R. Hanson, Quantum internet: A vision for the road ahead, *Science* **362**, eaam9288 (2018).
[3] N. Gisin, G. Ribordy, W. Tittel, and H. Zbinden, Quantum cryptography, *Reviews of Modern Physics* **74**, 145 (2002).
[4] R. Van Meter and S. J. Devitt, The path to scalable distributed quantum computing, *Computer* **49**, 31 (2016).
[5] D. Gottesman, T. Jennewein, and S. Croke, Longer-Baseline Telescopes Using Quantum Repeaters, *Physical Review Letters* **109**, 070503 (2012).
[6] P. Kómár, E. M. Kessler, M. Bishof, L. Jiang, A. S. Sørensen, J. Ye, and M. D. Lukin, A quantum network of clocks, *Nature Physics* **10**, 582 (2014).
[7] T. E. Northup and R. Blatt, Quantum information transfer using photons, *Nature Photonics* **8**, 356 (2014).
[8] S.-H. Wei, B. Jing, X.-Y. Zhang, J.-Y. Liao, C.-Z. Yuan, B.-Y. Fan, C. Lyu, D.-L. Zhou, Y. Wang, G.-W. Deng, H.-Z. Song, D. Oblak, G.-C. Guo, and Q. Zhou, Towards real-world quantum networks: A review, *Laser & Photonics Reviews* **16**, 2100219 (2022).
[9] S. Ritter, C. Nölleke, C. Hahn, A. Reiserer, A. Neuzner, M. Upho, M. Mücke, E. Figueroa, J. Bochmann, and G. Rempe, An elementary quantum network of single atoms in optical cavities, *Nature* **484**, 195 (2012).
[10] W. Rosenfeld, D. Burchardt, R. Garthoff, K. Redeker, N. Ortegel, M. Rau, and H. Weinfurter, Event-ready Bell test using entangled atoms simultaneously closing detection and locality loopholes, *Physical Review Letters* **119**, 010402 (2017).
[11] M. li Grimau Puigibert, M. F. Askarani, J. H. Davidson, V. B. Verma, M. D. Shaw, S. W. Nam, T. Lutz, G. C. Amaral, D. Oblak, and W. Tittel, Entanglement and nonlocality between disparate solid-state quantum memories mediated by photons, *Physical Review Research* **2**, 013039 (2020).
[12] N. Maring, P. Farrera, K. Kutluer, M. Mazzera, G. Heinze, and H. de Riedmatten, Photonic quantum state transfer between a cold atomic gas and a crystal, *Nature* **551**, 485-488 (2017).
[13] B. Jing, X.-J. Wang, Y. Yu, P.-F. Sun, Y. Jiang, S.-J. Yang, W.-H. Jiang, X.-Y. Luo, J. Zhang, X. Jiang, X.- H. Bao, and J.-W. Pan, Entanglement of three quantum memories via interference of three single photons, *Nature Photonics* **13**, 210 (2019).
[14] M. Pompili, S. L. N. Hermans, S. Baier, H. K. C. Beukers, P. C. Humphreys, R. N. Schouten, R. F. L. Vermeulen, M. J. Tiggelman, L. d. S. Martins, B. Dirkse, S. Wehner, and R. Hanson, Realization of a multi-node quantum network of remote solid-state qubits, *Science* **372**, 259 (2021).
[15] S. L. N. Hermans, M. Pompili, H. K. C. Beukers, S. Baier, J. Borregaard, and R. Hanson, Qubit teleportation between non-neighbouring nodes in a quantum network, *Nature* **605**, 663 (2022).
[16] M. D. Eisaman, J. Fan, A. Migdall, and S. V. Polyakov, Invited review article: Single-photon sources and detectors, *Review of Scientic Instruments* **82**, 071101 (2011).
[17] K. Heshami, D. G. England, P. C. Humphreys, P. J. Bustard, V. M. Acosta, J. Nunn, and B. J. Sussman, Quantum memories: Emerging applications and recent advances, *Journal of Modern Optics* **63**, 2005 (2016).
[18] N. Akopian, L. Wang, A. Rastelli, O. G. Schmidt, and V. Zwiller, Hybrid semiconductor-atomic interface: Slowing down single photons from a quantum dot, *Nature Photonics* **5**, 230 (2011).
[19] S. M. Ulrich, S. Weiler, M. Oster, M. Jetter, A. Urvoy, R. Löw, and P. Michler, Spectroscopy of the D_1 transition of cesium by dressed-state resonance fluorescence from a single (In,Ga)As/GaAs quantum dot, *Physical Review B* **90**, 125310 (2014).
[20] L. Zhai, G. N. Nguyen, C. Spinnler, J. Ritzmann, M. C. Löbl, A. D. Wieck, A. Ludwig, A. Javadi, and R. J. Warburton, Quantum interference of identical photons from remote GaAs quantum dots, *Nature Nanotechnology* **17**, 829 (2022).
[21] P. S. Michelberger, T. F. M. Champion, M. R. Sprague, K. T. Kaczmarek, M. Barbieri, X. M. Jin, D. G. England, W. S. Kolthammer, D. J. Saunders, J. Nunn, and I. A. Walmsley, Interfacing GHz-bandwidth heralded single photons with a warm vapour Raman memory, *New Journal of Physics* **17**, 043006 (2015).
[22] R. Mottola, G. Buser, C. Müller, T. Kroh, A. Ahlrichs, S. Ramelow, O. Benson, P. Treutlein, and J. Wolters, An efficient, tunable, and robust source of narrow-band photon pairs at the ^{87}Rb D_1 line, *Optics Express* **28**, 3159 (2020).
[23] S. Karlen, J. Gobet, T. Overstolz, J. Haesler, and S. Lecomte, Lifetime assessment of RbN_3-filled MEMS atomic vapor cells with Al_2O_3 coating, *Optics Express* **25**, 2187 (2017).
[24] J. Kitching, Chip-scale atomic devices, *Applied Physics Reviews* **5**, 031302 (2018).
[25] J.-M. Mol, L. Esguerra, M. Meister, D. E. Bruschi, A. W. Schell, J. Wolters, and L. Wörner, Quantum memories for fundamental science in space, *Quantum Science and Technology* **8**, 024006 (2023).
[26] M. Fleischhauer and M. D. Lukin, Quantum memory for photons: Dark-state polaritons, *Physical Review A* **65**, 022314 (2002).
[27] I. Novikova, R. Walsworth, and Y. Xiao, Electromagnetically induced transparency-based slow and stored light in warm atoms, *Laser & Photonics Reviews* **6**, 333 (2011).
[28] N. B. Phillips, A. V. Gorshkov, and I. Novikova, Light storage in an optically thick atomic ensemble under conditions of electromagnetically induced transparency and four-wave mixing, *Physical Review A* **83**, 063823 (2011).
[29] N. Lauk, C. O'Brien, and M. Fleischhauer, Fidelity of photon propagation in electromagnetically induced transparency in the presence of four-wave mixing, *Physical Review A* **88**, 013823 (2013).
[30] M. Yan, E. G. Rickey, and Y. Zhu, Electromagnetically induced transparency in cold rubidium atoms, *Journal of the Optical Society of America B* **18**, 1057 (2001).
[31] J. Wolters, G. Buser, A. Horsley, L. Béguin, A. Jöckel, J.-P. Jahn, R. J. Warburton, and P. Treutlein, Simple atomic quantum memory suitable for semiconductor quantum dot single photons, *Physical Review Letters* **119**, 060502 (2017).
[32] G. Buser, R. Mottola, B. Cotting, J. Wolters, and P. Treutlein, Single-photon storage in a ground-state vapor cell quantum memory, *PRX Quantum* **3**, 020349 (2022).
[33] R. Mottola, G. Buser, and P. Treutlein, Optical memory in a microfabricated rubidium vapor cell, *Physical Review Letters* **131**, 260801 (2023).
[34] M. Pellaton, C. Affolderbach, Y. Pétremand, N. de Rooij, and G. Mileti, Study of laser-pumped double-resonance clock signals using a microfabricated cell, *Physica Scripta* **T149**, 014013 (2012).
[35] R. Mottola, G. Buser, and P. Treutlein, Electromagnetically induced transparancy and optical pumping in the hyperfine Paschen-Back regime, *Physical Review A* **108**, 062820 (2023).
[36] F. S. Ponciano-Ojeda, F. D. Logue, and I. G. Hughes, Absorption spectroscopy and Stokes polarimetry in a ^{87}Rb vapour in the Voigt geometry with a 1.5 T external magnetic field, *Journal of Physics B: Atomic, Molecular and Optical Physics* **54**, 015401 (2021).
[37] A. V. Gorshkov, A. André, M. D. Lukin, and A. S. Sørensen, Photon storage in Λ-type optically dense atomic media. II. Free-space model, *Physical Review A* **76**, 033805 (2007).
[38] M. A. Rosenberry, J. P. Reyes, D. Tupa, and T. J. Gay, Radiation trapping in rubidium optical pumping at low buffer-gas pressures, *Physical Review A* **75**, 023401 (2007).
[39] S. E. Thomas, J. H. D. Munns, K. T. Kaczmarek, C. Qiu, B. Brecht, A. Feizpour, P. M. Ledingham, I. A. Walmsley, J. Nunn, and D. J. Saunders, High efficiency Raman memory by suppressing radiation trapping, *New Journal of Physics* **19**, 063034 (2017).
[40] H. Chi, W. Quan, J. Zhang, L. Zhao, and J. Fang, Advances in anti-relaxation coatings of alkali-metal vapor cells, *Applied Surface Science* **501**, 143897 (2020).
[41] O. Katz and O. Firstenberg, Light storage for one second in room-temperature alkali vapor, *Nature Communications* **9**, 2074 (2018).

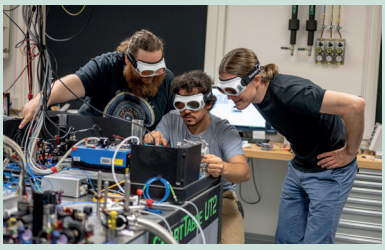

Gianni Buser and **Roberto Mottola** are postdoctoral researchers in the Quantum Memory Lab at the University of Basel, working in the research group of Prof. **Philipp Treutlein**. Over the past few years, they built a quantum memory for light using hot atomic vapors as storage medium, demonstrating single-photon storage and retrieval with high bandwidth. Their current research is focused on optimizing and miniaturizing such quantum memories and interfacing them with high-quality single-photon sources such as semiconductor quantum dots and spontaneous parametric downconversion sources. Demonstrating elementary quantum interconnects on a scalable technological platform will be an important step towards quantum networking demonstrations, such as entanglement distribution between multiple network nodes.